Proc. Natl. Acad. Sci. USA
Vol. 92, pp. 10496–10500, November 1995
Medical Sciences

Molecular basis of human mitochondrial very-long-chain acyl-CoA dehydrogenase deficiency causing cardiomyopathy and sudden death in childhood

(β-oxidation/metabolism/fatty acids/Reye syndrome/genetic defect)

ARNOLD W. STRAUSS*†‡, CYNTHIA K. POWELL*, DANIEL E. HALE§, MELISSA M. ANDERSON*, AJAY AHUJA*, JEFFREY C. BRACKETT¶, AND HAROLD F. SIMS*

Departments of *Pediatrics, †Molecular Biology and Pharmacology, and ¶Medicine, Washington University School of Medicine and St. Louis Children's Hospital, St. Louis, MO 63110; and §Department of Pediatrics, University of Texas–San Antonio, San Antonio, TX 78284

Communicated by William H. Daughaday, Balboa Island, CA, July 3, 1995

ABSTRACT **β-Oxidation of long-chain fatty acids provides the major source of energy in the heart. Defects in enzymes of the β-oxidation pathway cause sudden, unexplained death in childhood, acute hepatic encephalopathy or liver failure, skeletal myopathy, and cardiomyopathy. Very-long-chain acyl-CoA dehydrogenase [VLCAD; very-long-chain-acyl-CoA:(acceptor) 2,3-oxidoreductase, EC 1.3.99.13] catalyzes the first step in β-oxidation. We have isolated the human VLCAD cDNA and gene and determined the complete nucleotide sequences. Polymerase chain reaction amplification of VLCAD mRNA and genomic exons defined the molecular defects in two patients with VLCAD deficiency who presented with unexplained cardiac arrest and cardiomyopathy. In one, a homozygous mutation in the consensus dinucleotide of the donor splice site ($g^{+1} \rightarrow a$) was associated with universal skipping of the prior exon (exon 11). The second patient was a compound heterozygote, with a missense mutation, $C^{1837} \rightarrow T$, changing the arginine at residue 613 to tryptophan on one allele and a single base deletion at the intron–exon 6 boundary as the second mutation. This initial delineation of human mutations in VLCAD suggests that VLCAD deficiency reduces myocardial fatty acid β-oxidation and energy production and is associated with cardiomyopathy and sudden death in childhood.**

Very-long-chain acyl-CoA dehydrogenase (VLCAD) catalyzes the first step in the mitochondrial β-oxidation spiral that supplies the majority of energy in mature heart and is crucial to intermediary metabolism in the liver (1–3). This spiral requires four enzymatic activities, an initial fatty acyl-CoA dehydrogenase, a 2,3-enoyl-CoA hydratase reaction, a 3-hydroxy-acyl-CoA dehydrogenase step, and the final 3-ketoacyl-CoA thiolase cleavage step. Because fatty acids with different chain lengths are substrates in these reactions, several enzymes, encoded by distinct nuclear genes, are required for each step. For the initial fatty acyl-CoA dehydrogenase step, four enzymes with overlapping, but different, chain length specificities have been identified and designated as VLCAD, which acts on substrates of 14–20 carbons in length (1); long-chain acyl-CoA dehydrogenase (LCAD); medium-chain acyl-CoA dehydrogenase (MCAD); and short-chain acyl-CoA dehydrogenase (SCAD). Biochemical characterization of the last three soluble, matrix enzymes (4) revealed similar structures consisting of four identical 42-kDa subunits and FAD as a cofactor. The cloning of mRNAs encoding the subunits of MCAD, LCAD, and SCAD revealed similarity of their primary sequences (5, 6). The discovery, characterization, and cloning of rat VLCAD (1) demonstrated significant differences from the other three members of this CAD family. VLCAD is a homodimer of 70-kDa subunits and is associated with the inner mitochondrial membrane.

The importance of the β-oxidation pathway for energy production is emphasized by inherited deficiencies of these enzyme activities (2, 3). Individuals with these disorders frequently become critically ill in infancy after a period of reduced caloric intake and may present with a Reye-like syndrome of hypoglycemia, fatty liver, and coma; sudden, unexplained death; skeletal myopathy; or cardiomyopathy.

Based upon enzyme assay studies with palmitoyl-CoA as a substrate, it was suggested that LCAD deficiency was the β-oxidation enzyme defect most commonly associated with cardiomyopathy (3, 7). However, molecular studies of LCAD in these patients did not demonstrate any mutations (8). With the biochemical evidence that VLCAD (1) produces most of the activity in fibroblasts measured with palmitoyl-CoA substrate, these patients were reexamined by protein blotting studies with the conclusion that some individuals previously considered as LCAD-deficient really were deficient in VLCAD (8, 9).

These results prompted us to search for VLCAD mutations in such patients. Here we provide the molecular genetic characterization of mutations in two patients with recessively inherited VLCAD deficiency associated with infantile cardiomyopathy and sudden death.‖

MATERIALS AND METHODS

Cell Lines, Enzyme Assays, DNA Isolation, and RNA Isolation. Maintenance of skin fibroblasts and isolation of RNA and DNA were done as described (10). VLCAD activity in whole cell extracts was measured (7) with palmitoyl-CoA as the substrate.

VLCAD cDNA Isolation and Characterization. Oligonucleotide primers (0.5 μM) corresponding to the rat VLCAD cDNA (1) (sense, bp 1146–1175; antisense, bp 1686–1712) were used to amplify this 567-bp segment with total DNA isolated from a rat cardiac cDNA library as the template for PCR. This rat VLCAD cDNA fragment was then used to screen 300,000 plaques of a human heart cDNA library prepared in the λ ZAPII vector (Stratagene). To identify phage clones containing the 5′ end of human heart VLCAD cDNA, we developed a rapid PCR screening strategy. Aliquots

The publication costs of this article were defrayed in part by page charge payment. This article must therefore be hereby marked "*advertisement*" in accordance with 18 U.S.C. §1734 solely to indicate this fact.

Abbreviations: UTR, untranslated region; LCAD, long-chain acyl-CoA dehydrogenase; MCAD, medium-chain acyl-CoA dehydrogenase; SCAD, short-chain acyl-CoA dehydrogenase; VLCAD, very-long-chain acyl-CoA dehydrogenase; SSCV, single-strand conformation variance.

‡To whom reprint requests should be addressed.

‖The sequence reported in this paper has been deposited in the GenBank data base [accession no. L46590 (genomic)].

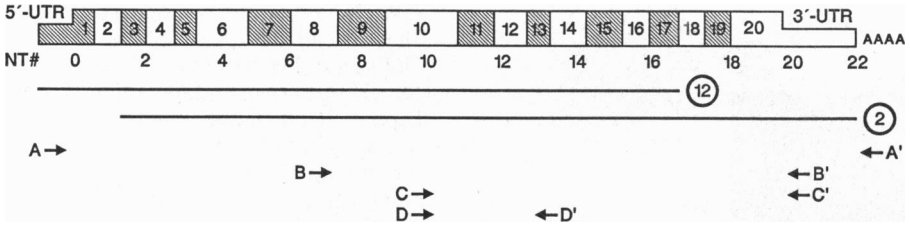

FIG. 1. Structure of human VLCAD mRNA. Lengths of human heart cDNA clones labeled 2 and 12 are indicated by the lines. This figure is a scale diagram of the VLCAD mRNA structure with the 3′ and 5′ untranslated regions (UTRs) depicted in smaller boxes and the coding region shown as the larger box containing numbered exons of the sizes and boundaries shown. NT# indicates the nucleotide number (in hundreds), beginning with the start codon. Letters with arrows show the locations of primer pairs used in PCR amplification of VLCAD mRNA.

of phage DNA from 5-mm agarose plugs taken from the primary plates and containing plaques reactive with the rat VLCAD mid-coding-region probe (bp 1146–1712) were subjected to PCR amplification with oligonucleotides corresponding to bp 229–254 (sense) and bp 421–446 (antisense) of rat VLCAD. This PCR step identified clones which must span the VLCAD coding region from about bp 350 to bp 1650. The doubly positive clones (Fig. 1, labeled 2 and 12) with the largest inserts were subjected to complete nucleotide sequence analyses by the dideoxy chain-termination method.

VLCAD Gene Isolation and Characterization. The rat 5′ oligonucleotide primers were also used with human genomic DNA as a template to amplify this portion of the human VLCAD gene. The amplified product was 400 bp long, some 200 bp larger than the corresponding cDNA fragment (bp 229–446). Sequence analysis documented that this fragment contained portions of three exons and the two small intervening introns. With this sequence, we designed two oligonucleotides for PCR-based screening of a human genomic P1 plasmid library (Genome Systems St. Louis) (11). The sense primer was bp 229–254 of the VLCAD coding region and the antisense primer (5′-aaggcacaggatcccacatccaggctc) was from the downstream intron. A single purified P1 clone was isolated and characterized by restriction enzyme digestion and Southern blot analysis. The complete nucleotide sequence of the entire gene was done on both strands of overlapping restriction fragments.

PCR Amplification of Mutant Human VLCAD cDNA and PCR Amplification and Single-Strand Conformation Variance (SSCV) Analysis of Human VLCAD Exons. Amplification of fibroblast RNA was performed by PCR using cDNA template and a sense oligonucleotide corresponding to bp −51 to −25 and oligo(dT) as the antisense primer (Fig. 1, A and A′, respectively) in the first reaction. An aliquot was then used as the template for a second round of amplification with three sets of internal primers. PCR amplification of genomic DNA was done with intronic primer pairs containing engineered restriction sites (underlined): exon 11, sense, 5′-cctagggagactgcggatccacactga; exon 11, antisense, 5′-gggaagaaacgcccagggatccaggga; exons 5–6, sense, 5′-ccagcctggtacctgaccagcctg; exons 5–6, antisense, 5′-catactgggatgtgcggtaccgggcgc; exon 20, sense, 5′-caggcccaacccctcaagcttccctct; and exon 20, antisense, 5′-cctggccgggagtaagcttcagaag, bp 1962–1983 of human VLCAD cDNA.

The amplified products were analyzed for SSCV by nondenaturing gel electrophoresis (12), or were subjected to direct sequence analysis, or were placed into plasmid vectors and complete nucleotide sequences of multiple subclones were obtained.

RESULTS AND DISCUSSION

Characterization of Human VLCAD cDNA. To study the molecular basis of human VLCAD deficiency, we first determined the complete sequence of human VLCAD cDNA. We used primer sequences from the published rat VLCAD cDNA (1) to generate PCR-amplified probes for screening of a human heart cDNA library. Two overlapping clones (Fig. 1) provided the human heart VLCAD cDNA sequence, which is 2250 bp long and includes 88 bp of 5′ UTR, 1965 bp of coding region, 171 bp of 3′ UTR, and a poly(A) tail. The derived protein sequence of 655 aa includes a 40-aa transit peptide, rich in arginine (7 of 40 aa) and lacking acidic residues, required for import into mitochondria. Within the mature protein of 615 aa, a region of homology (about 30% similarity) to the acyl-CoA dehydrogenases extends from aa 90 to aa 475 and includes a glutamic residue at position 462, homologous to the proton-abstracting active site glutamate at position 376 of human MCAD (6, 13). In MCAD, Trp^{166} is likely important in electron transfer from FAD to electron transfer flavoprotein (14). The corresponding tryptophan in human VLCAD, Trp^{249}, and the adjacent residues are also highly conserved among the acyl-CoA dehydrogenases. Human VLCAD and rat VLCAD (1) are quite similar, with 85% nucleotide sequence identity and 87% amino acid identity in the coding region. The carboxyl-terminal 170 aa, which are not present in the other acyl-CoA dehydrogenases, are highly conserved across species (86% identity), consistent with an important functional role in membrane association or in dimer formation.

Structural Characterization of the Human VLCAD Gene. To allow detailed molecular genetic studies and for subsequent studies of gene regulation, we isolated a P1 clone containing

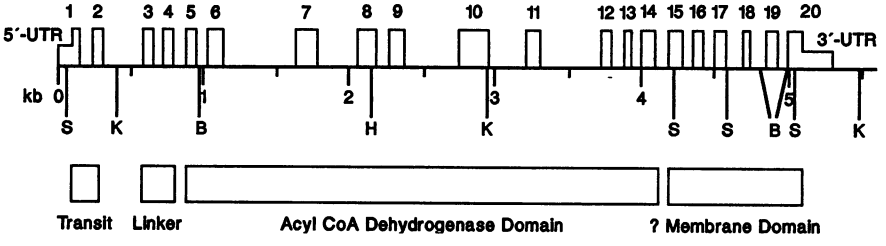

FIG. 2. Structure and organization of the human VLCAD gene. At the top of the scaled diagram are numbers above boxes indicating the positions of exons. The shorter boxed regions are the 5′ and 3′ UTRs, as indicated. The numbers below the line show the length of the gene in kilobases, beginning with the presumed transcription start site. Positions of restriction enzyme recognition sites are designated: S, *Sac* I; K, *Kpn* I; B, *Bam*HI; H, *Hin*dIII. The four boxes at the bottom indicate VLCAD functional domains. The question mark suggests that the role of the VLCAD carboxyl-terminal amino acids encoded by exons 15–20 in binding to mitochondrial membranes is not proven.

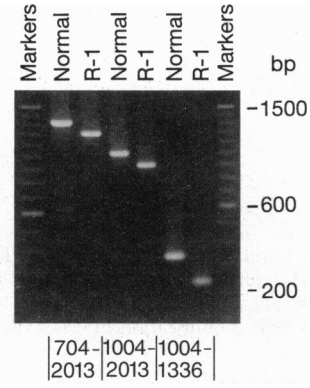

FIG. 3. PCR amplification of total RNA isolated from fibroblasts derived from patient R-1 or from a normal individual reveals a 105-bp deletion in R-1. PCR was performed first with primer set A/A′ (Fig. 1) and then in a second reaction with primer sets B/B′, C/C′, or D/D′ (see Fig. 1) (at the nucleotide positions of VLCAD mRNA indicated at the bottom). The products were then analyzed by 1.5% agarose gel electrophoresis simultaneously with marker DNA of the sizes indicated at right. With all three primer sets, the product derived from R-1 fibroblast RNA is smaller by about 100 bp than that derived from normal RNA.

the entire human VLCAD gene and determined its complete nucleotide sequence (Figs. 1 and 2). The VLCAD gene is compact, with exactly 5340 bp from the presumed transcription start site to the site of poly(A) addition. Only 58% of the gene is comprised by introns. By comparison with the VLCAD cDNA, we defined 20 exons, ranging in size from 63 to 309 bp. The largest intron is only 459 bp long, with the shortest being 71 bp. Exons 12–20 are very closely spaced, with similar lengths (63–102 bp), and are separated by similarly sized, small introns (71–95 bp). The splice junction sequences at 19 of the 20 exon–intron boundaries compare well with the consensus donor and acceptor sequences (15). The donor splice sequence after exon 8 is gcaacct, which violates the gt dinucleotide and gta/gagt splice donor consensus sequences. However, gc is present at the donor site of a few normal exons (15).

Delineation of the VLCAD Molecular Defect in Family R. With our human VLCAD mRNA and gene structural data, we began characterizing mutations in VLCAD-deficient individuals. The original reports (7, 16) of deficient mitochondrial dehydrogenase activity against palmitoyl-CoA contain the history of patient R-1. This infant, the child of parents who are distant cousins, had two unexplained cardiac arrests in the first 10 weeks after birth, the second associated with hypoglycemia and severe hypertrophic cardiomyopathy. The child, now 13, remains developmentally delayed with frequent episodes of hypoglycemia and transient muscle weakness provoked by fasting or illness. No immunoreactive VLCAD protein was detected in his fibroblast extracts (8), and biosynthetic studies demonstrate rapid degradation of a slightly smaller, immunoreactive mutant VLCAD (9).

To elucidate the molecular defect in VLCAD in this patient, we used PCR amplification of VLCAD mRNA from his cultured fibroblasts with primer set A/A′ (Fig. 1). Nested PCR with three sets of internal primers (shown in Fig. 1 as B/B′, C/C′, and D/D′) yielded amplified products derived from fibroblast RNA of patient R-1 that were smaller by about 100 bp than the products amplified from VLCAD fibroblast RNA of a normal person (Fig. 3). No product of normal size was detected after amplification of patient R-1's RNA, indicating a universal deletion in the mutant VLCAD mRNA between bp 1029 and bp 1313. Multiple sequence analyses (data not shown) revealed a 105-bp deletion, corresponding precisely to exon 11 (bp 1078–1182) (Fig. 1), in all clones analyzed. Thus, all of patient R-1's fibroblast VLCAD mRNA detected with this sensitive method exhibited skipping of exon 11, which encodes precisely 35 aa within the region of VLCAD homologous to the other acyl-CoA dehydrogenases.

This result suggested that a splice-site abnormality might be the causative mutation. Because the parents are consanguineous, a homozygous mutation was possible. We used intronic primers encompassing exon 11 to amplify genomic DNA from the patient, both parents, and his asymptomatic brother (Fig. 4). Analysis of the products by SSCV and comparison with the PCR fragment derived from normal genomic DNA revealed that the mother, father, and brother shared some bands with the normal, but also had aberrantly migrating bands. This is consistent with heterozygosity for a nucleotide difference. Product from the affected child, R-1, did not contain one of the normal conformers but did share the aberrantly migrating band with members of his family, consistent with homozygosity for the same mutation. Direct sequence analysis (Fig. 4) of all four family members revealed that R-1 was homozygous for a mutation at the first nucleotide of the donor splice site after exon 11, a $g^{+1} \rightarrow$ a change. His parents and brother were heterozygous for this mutation. This mutation alters the highly conserved consensus dinucleotide of the donor splice site from GAGgtgag to GAGatgag.

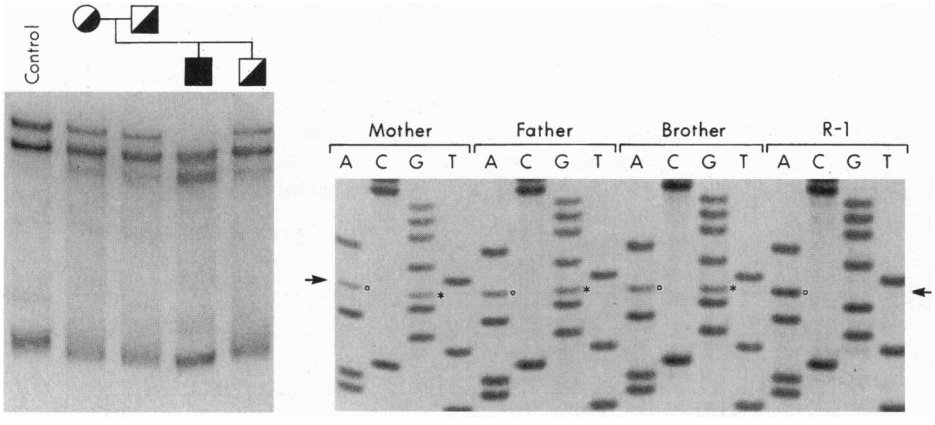

FIG. 4. Delineation of exon 11 splice donor-site mutation, $g^{+1} \rightarrow$ a, in family R. PCR amplification of genomic DNA from individual R-1, his parents, his sibling, and a normal individual was performed with intronic primers flanking exon 11. (*Left*) SSCV analysis of amplified exon 11 DNA. A diagram of the family is presented at the top, and the amplified exon 11 DNA from each individual in the family is shown in the lane directly below each symbol. The normal control is the first lane. (*Right*) Direct sequence analysis of amplified exon 11 DNA for all four members of the family. Arrow indicates the position of the altered nucleotide. The genomic sequence from the mother, father, and sibling has two bands, the normal G (shown by an asterisk to the right of the band) and the mutant A (shown by a circle), indicating that all three are heterozygous at this site. Amplified DNA from individual R-1 has only the mutant A at this intronic +1 position. Thus, he is a homozygous mutant.

Mutations in donor splice sites of other genes cause exon skipping. For example, we detected (10) two different mutations in a single individual with long-chain 3-hydroxyacyl-CoA dehydrogenase deficiency at the +1 and +3 positions of the same donor splice site which caused universal skipping of the prior exon. Other examples (17–20) include mutations in donor splice sites of the lipoprotein lipase, phosphofructokinase, β-spectrin, and ornithine carbamoyltransferase genes which cause either skipping of the previous exon or use of alternative, cryptic splice sites.

Skipping of exon 11 in this patient creates a mutant VLCAD mRNA lacking 105 bp, encoding the 35 aa homologous to residues 274–308 of mature human MCAD (5). In the MCAD structure, these amino acids are in the carboxyl-terminal helical region (14), in the midst of the acyl-CoA dehydrogenase domain. It is likely that the expressed mutant protein either could not be transported into mitochondria or could not fold properly, resulting in rapid degradation of the mutant VLCAD. This would be consistent with the reported (9) protein synthetic studies and the lack of immunoreactive VLCAD protein (8) in this patient's fibroblasts.

Characterization of Two Mutant VLCAD Alleles in Family A. The original report (7) describes the affected child, A-1, in this family. She presented at 4 months of age with vomiting, lethargy, hypotonia, and a subsequent respiratory arrest. Laboratory testing revealed hypoketotic hypoglycemia and significant cardiac hypertrophy and dysfunction. She improved with frequent high carbohydrate feedings but died suddenly 2 months later during a viral illness. Previous reports document very low dehydrogenase activity with C_{16}-CoA substrate (7), reduced VLCAD protein antigen in her fibroblast extracts (8), and rapid degradation of her normal-sized, mutant VLCAD protein (9).

To define the presumed VLCAD mutations in this patient, we amplified all 20 of her exons for subsequent SSCV analysis. Two of the amplified exonic products revealed differences from normal (Fig. 5). The exon 20 fragment amplified from genomic DNA of individual A-1, her brother, and her mother (Fig. 5 *Left*) showed a different banding pattern than the normal control, consistent with a heterozygous difference. The pattern of conformers was normal for the exon 20 genomic fragment derived from her father and sister. Sequence analyses (Fig. 5 *Center*) of A-1's exon 20 DNA revealed a single base difference at nt 1837, a C → T change, predicting a change in VLCAD residue 613 from Arg to Trp that substitutes a bulky hydrophobic side chain for a positively charged one. This mutation lies within the region of VLCAD which is not shared with the other CADs and which may be important in dimer formation or interaction with mitochondrial membranes. A potential consequence of this mutation in expressed VLCAD might be rapid degradation secondary to improper localization or folding, consistent with the pulse–chase studies in her fibroblasts (9).

Analysis (not shown) of exon 5–6 conformers revealed that A-1 had different bands from normal, although other bands were similar to the normal conformers. This is consistent with heterozygosity for a nucleotide difference. Sequence analysis of multiple exon 5–6 subclones from A-1 (Fig. 5 *Right*) revealed deletion of one of the two guanine nucleotides forming the intron–exon 6 boundary. The normal sequence is ccccag-GAA, and the mutant sequence is ccccaGAA. The most likely consequence of this deletion would be an alteration in splicing because of loss of the conserved ag dinucleotide at the splice acceptor site (15). Alternatively, splicing at this site might occur, but this would result in loss of a single nucleotide in exon 6, causing a shift in the mRNA reading frame. In either event, this mutation would most likely result in an unstable mRNA and lack of VLCAD protein expression from this mutant allele.

VLCAD Deficiency Correlates with Pediatric Cardiomyopathy. Our results demonstrate that these two patients, previously believed to have LCAD deficiency, actually have molecular defects in their VLCAD genes. In both, one phenotypic characteristic was cardiomyopathy. Cardiomyopathy in infants and children has usually been ascribed to myocarditis. However, recent clinical studies reveal familial occurrence in 30% (21), and molecular studies have proved the genetic nature of cardiomyopathy in some patients (22). For example, dominantly inherited hypertrophic cardiomyopathy (23) is caused by mutations in genes encoding three cardiac contractile proteins: α-cardiac myosin heavy chain, α-tropomyosin, and cardiac troponin T. A prominent feature of Becker muscular dystrophy is dilated cardiomyopathy. This X chromosome-linked disease is caused by defects in dystrophin, a subsarcolemmal structural protein linked to the extracellular matrix by a complex of associated proteins (22).

Our results demonstrate that, in addition to causative mutations in contractile proteins, hypertrophic cardiomyopathy in infants is associated with defects in VLCAD, an enzyme

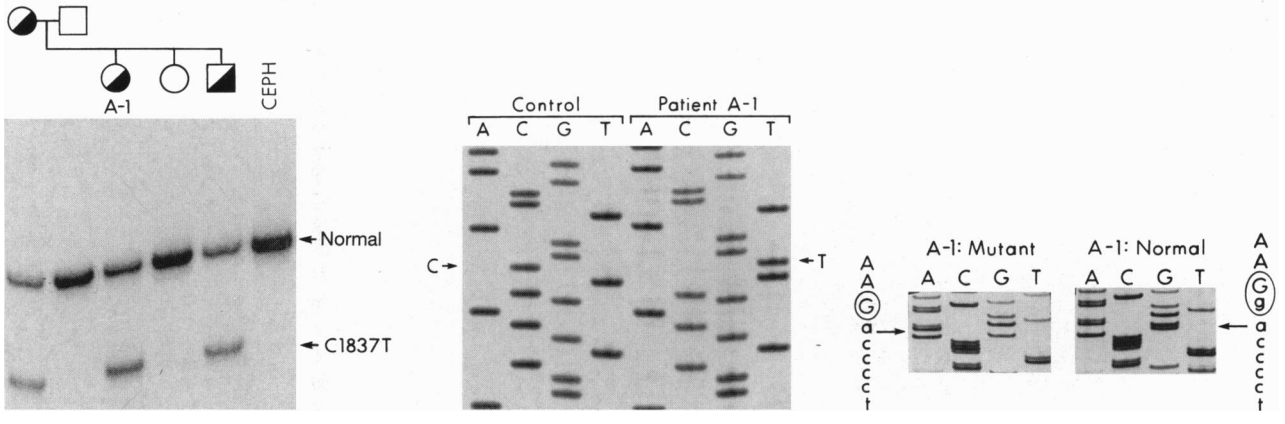

FIG. 5. Delineation of the two mutations in patient A-1. Genomic DNA from individual A-1, her parents, her two siblings, and a normal person was amplified with oligonucleotides flanking the exon 20 coding region. (*Left*) SSCV analysis of the PCR products. A diagram of the family relationships is shown above the gel autoradiograph, with each individual directly above the lane with their amplified exon 20 products. The exon 20 sample in the far right lane is from a normal individual (labeled CEPH). Exon 20 amplified DNA from the mother, patient A-1, and her brother has aberrantly migrating bands, indicating heterozygosity for the $C^{1837} \rightarrow T$ mutation. (*Center*) DNA sequence of subclones of exon 20 amplified DNA. The control sequence shows the normal C; the sequence of patient A-1 has the mutant T. Among eight exon 20 subclones, individual A-1 had the normal C; in four and the mutant T in four; thus A-1 is heterozygous for this $C^{1837} \rightarrow T$ mutation. (*Right*) Partial sequences of two subclones from exon 5–6 amplified DNA from patient A-1. One of the two guanines forming the intron–exon 6 boundary is absent in the A-1 mutant sequence, but the normal sequence is present in A-1 normal lanes, confirming heterozygosity at this position.

essential for myocardial energy production. We have also delineated a molecular defect in the gene encoding the α subunit of trifunctional protein in a toddler dying suddenly with dilated cardiomyopathy (10). Trifunctional protein is a complex that catalyzes three steps in β-oxidation of long-chain fatty acids in mitochondria. Defects in MCAD and 3-ketoacyl-CoA thiolase, other enzymes of the β-oxidation spiral, cause sudden, unexplained death or cardiomyopathy (22). In addition, mutations in the maternally inherited mitochondrial genome may cause dilated or hypertrophic cardiomyopathy (22). Mitochondria in these patients also have reduced capacity for energy production because of loss of subunits of respiratory-chain complexes. We speculate that cardiac hypertrophy or dilatation with poor function represents responses to inadequate energy supply, secondary to mitochondrial protein deficiencies, either in the β-oxidation pathway or in the respiratory chain. With fasting, defects in enzymes which break down long-chain fatty acids also result in dramatic tissue accumulation of long-chain fatty acylcarnitines (2, 3). These compounds are toxic to mitochondria and can cause lethal ventricular arrhythmias. Together, these molecular studies prove that cardiomyopathy and sudden, unexplained death are frequently manifestations of molecular defects in proteins required for contraction or energy production in the heart.

SUMMARY AND CONCLUSIONS

We present complete structural characterizations of the human VLCAD cDNA and gene, which were used to delineate the mutations in two individuals with VLCAD deficiency. One individual has a homozygous splice donor-site mutation causing exon skipping and protein instability. By positron emission tomography with labeled palmitic acid, this individual has been shown to have a reduced capacity for fatty acid oxidation in the heart (24). The second patient, who died suddenly, is a compound heterozygote for a splice acceptor-site mutation and a missense mutation, $Arg^{613} \rightarrow Trp$. Discovery of these mutations in the VLCAD gene in two individuals previously thought to have LCAD deficiency proves definitively that these two patients actually have VLCAD deficiency and emphasizes the importance of molecular characterization of mutations and the redundancy in enzymatic activities in the β-oxidation spiral. VLCAD deficiency is thus firmly linked to the phenotype of cardiomyopathy and sudden, unexplained death. These phenotypes are consistent with the crucial role of long-chain fatty acid β-oxidation for energy production in the heart.

We thank Daniel Kelly and R. Mark Payne for critical review of the manuscript. This work was supported by National Institutes of Health Grants P01-DK33487 (A.W.S.), T32-HL07081 (J.C.B.), and HD24061 (the Kennedy/Hopkins Mental Retardation Research Center Core Grant).

1. Aoyama, T., Ueno, I., Kamijo, T. & Hashimoto, T. (1994) *J. Biol. Chem.* **269,** 19088–19094.
2. Hale, D. E. & Bennett, M. J. (1992) *J. Pediatr.* **121,** 1–11.
3. Roe, C. R. & Coates, P. M. (1995) in *The Metabolic Basis of Inherited Disease*, eds. Scriver, C. R., Beaudet, A. L., Sly, W. S. & Valle, D. (McGraw-Hill, New York), pp. 1501–1533.
4. Ikeda, Y., Keese, S. M., Fenton, W. A. & Tanaka, K. (1987) *J. Biol. Chem.* **260,** 1311–1325.
5. Kelly, D. P., Kim, J.-J., Billadello, J. J., Hainline, B. E., Chu, T. W. & Strauss, A. W. (1987) *Proc. Natl. Acad. Sci. USA* **84,** 4068–4072.
6. Matsubara, Y., Indo, Y., Naito, E., Ozasa, H., Glassberg, R., Vockley, J., Ikeda, Y., Kraus, J. & Tanaka, K. (1989) *J. Biol. Chem.* **264,** 16321–16331.
7. Hale, D. E., Batshaw, M. L., Coates, P. M., Frerman, F. E., Goodman, S. I., Singh, I. & Stanley, C. A. (1985) *Pediatr. Res.* **19,** 666–671.
8. Yamaguchi, S., Indo, Y., Coates, P. M., Hashimoto, T. & Tanaka, K. (1993) *Pediatr. Res.* **34,** 111–113.
9. Aoyama, T., Souri, M., Ushikubo, S., Kamijo, T., Yamaguchi, S., Kelley, R. I., Rhead, W. J., Uetake, K., Tanaka, K. & Hashimoto, T. (1995) *J. Clin. Invest.* **95,** 2465–2473.
10. Brackett, J. C., Sims, H. F., Rinaldo, P., Shapiro, S., Powell, C. K., Bennett, M. J. & Strauss, A. W. (1995) *J. Clin. Invest.* **95,** 2076–2082.
11. Sternberg, N. (1990) *Proc. Natl. Acad. Sci. USA* **87,** 103–107.
12. Orita, M., Iwahana, H., Kanazawa, H., Hayashi, K. & Sekiya, T. (1989) *Proc. Natl. Acad. Sci. USA* **86,** 2766–2770.
13. Bross, P., Engst, S., Strauss, A. W., Kelly, D. P., Rasched, I. & Ghisla, S. (1990) *J. Biol. Chem.* **265,** 7116–7119.
14. Kim, J.-J., Wang, M. & Paschke, R. (1993) *Proc. Natl. Acad. Sci. USA* **90,** 7523–7527.
15. Senapathy, P., Shapiro, M. B. & Harris, N. L. (1990) *Methods Enzymol.* **183,** 252–270.
16. Amendt, B. A., Moon, A., Teel, L. & Rhead, W. J. (1988) *Pediatr. Res.* **23,** 603–605.
17. Gotoda, T., Yamada, N., Murase, T., Inaba, T., Ishibashi, S., Shiman, H., Koga, S., Yazaki, Y., Furuichi, T. & Takaku, F. (1991) *J. Biol. Chem.* **266,** 24757–24762.
18. Raben, N., Sherman, J., Miller, F., Mena, H. & Plotz, P. (1993) *J. Biol. Chem.* **268,** 4963–4967.
19. Garbarz, M., Tse, W. T., Gallagher, P. G., Picat, C., Lecomte, M.-C., Galibert, F., Dhermy, D. & Forget, B. G. (1991) *J. Clin. Invest.* **88,** 76–81.
20. Carstens, R. P., Fenton, W. A. & Rosenberg, L. R. (1991) *Am. J. Hum. Genet.* **48,** 1105–1114.
21. Michels, V. V., Moll, P. P., Miller, F. A., Tajik, F., Chu, J. S., Driscoll, D. J., Burnett, J. C., Rodeheffer, R. J., Chesebro, J. H. & Tazelaar, H. D. (1992) *N. Engl. J. Med.* **326,** 77–82.
22. Kelly, D. P. & Strauss, A. W. (1994) *N. Engl. J. Med.* **330,** 913–919.
23. Watkins, H., McKenna, W. J., Thierfelder, L., Suk, H. J., Anan, R., O'Donoghue, A., Spirito, P., Matsumori, A., Moravec, C. S., Seidman, J. G. & Seidman, C. E. (1995) *N. Engl. J. Med.* **332,** 1058–1064.
24. Kelly, D. P., Mendelsohn, N. J., Sobel, B. E. & Bergmann, S. R. (1993) *Am. J. Cardiol.* **71,** 731–744.